Magnetic Correlations in the Zn-Mg-Rare-Earth Icosahedral Quasicrystals

Taku J Sato, Hiroyuki Takakura, An Pang Tsai, Kenji Ohoyama[1], Kaoru Shibata[1] and Ken H Andersen[2*]

National Research Institute for Metals, Tsukuba 305-0047, Japan[†]
and CREST, Japan Science and Technology Corporation, Saitama 332-0012, Japan
[1] *Institute for Materials Research, Tohoku University, Sendai 980-8577, Japan*
[2] *Institut Laue Langevin, BP 156, F-38042, Grenoble Cedex 9, France*

Received

Abstract

The previously-reported magnetic long-range order has been revisited in the Zn-Mg-rare-earth systems by means of the neutron diffraction, magnetic susceptibility and microstructural analysis. It was found that the long-range order is absent in icosahedral quasicrystals, where only short-range spin correlations develop even at the lowest temperatures. The long-range order was attributed to the $(Zn_xMg_{1-x})_5RE$ crystalline phase, which was shown to be a contaminating phase in the previously-used samples. The short-range spin correlations have been investigated in detail by single-quasicrystal neutron scattering. A close relation has been suggested between the short-range correlations and the quasiperiodic structure.

Keywords: Zn-Mg-RE system, neutron scattering, short-range spin correlations

1. Introduction

The Zn-Mg-rare-earth (RE) icosahedral quasicrystals are quite unique among known quasicrystals: they contain well-localized RE magnetic moments (spins) [1, 2, 3]. Thus, the quasicrystals enable us to study behavior (ordering) of spins in the quasiperiodic structure.

So far, magnetic properties of the Zn-Mg-RE quasicrystals have been reported by several groups. Exemplified by the RE = Ho system, magnetic susceptibility shows a paramagnetic increase as temperature is decreased. It perfectly obeys the Curie-Weiss law at high temperatures [4, 5, 6, 7, 8]. The estimated effective moment is almost equal to that of a Ho^{3+} free ion. The magnetic susceptibility starts to deviate from the Curie-Weiss law below about 6 K [7]. The deviation is very small, suggesting a development of weak spin correlations and/or (quasi)crystalline-electric-field splitting. Then, it abruptly shows spin-glass-like freezing at $T_f \sim 2$ K. Magnetic susceptibilities of the other RE quasicrystals behave quite similarly except for difference in temperature scale. The spin-glass-like freezing was also detected in ac susceptibility [6, 8] and μSR relaxation rate [9]. From the above results, one might conclude that the spins are randomly frozen at the lowest temperature in the Zn-Mg-RE quasicrystals as seen in canonical spin-glass systems.

On the other hand, the powder neutron diffraction by Charrier *et al.* [10] detected magnetic long-range order (magnetic Bragg reflections), coexisting with diffuse scattering. Both of the scattering simultaneously developed below T_N, where $T_N \simeq 7$ K for the Ho system. From this result, they concluded that the magnetic long-range order is established below T_N. However, the long-range order is consistent neither with the susceptibility, nor with the μSR result. They performed the neutron diffraction

*Present Address: ISIS facility, Rutherford Appleton Laboratory, Chilton, Didcot, Oxfordshire OX11 0QX, U.K.
†Corresponding address.

with $Zn_{50}Mg_{42}RE_8$ alloys. However, recent metallographic surveys showed that the alloys can probably be contaminated by crystalline phases, and ideal composition of the icosahedral quasicrystals is almost $Zn_{60}Mg_{30}RE_{10}$[11, 12]. Indeed, two later studies revealed that single icosahedral-phased samples exhibit only the diffuse scattering part of the first work [13, 14].

In this work, we aimed to clarify the origin of the previously-reported magnetic long-range order in the Zn-Mg-RE alloys. We have shown that the long-range order originates from the crystalline contamination in the previously-used alloys, and that intrinsic magnetic order in the icosahedral quasicrystals is the spin-freezing with significant short-range spin correlations. The short-range correlations have been investigated in details by the single-quasicrystal neutron scattering. A part of the present study was already published in Refs.[14, 15].

2. Experimental

Polycrystalline alloys of $Zn_{60}Mg_{30}RE_{10}$, $Zn_{50}Mg_{42}RE_8$ and $Zn_{68}Mg_{16}RE_{16}$ ($(Zn_{0.8}Mg_{0.2})_5RE$) for RE = Tb, Dy, Ho and Er were prepared by melting constituent elements in an induction furnace using pure Al_2O_3 crucibles. Purities of the starting materials were 99.9999%, 99.99% and 99.9% for Zn, Mg, and RE, respectively. The alloys were wrapped in Mo foils, sealed in Pyrex or quartz tubes, and annealed under several conditions. They were characterized by scanning and transmission electron microscopies (SEM and TEM) and X-ray diffraction. Compositions of phases in the alloys were determined by measuring energy-dispersive X-ray spectra in the SEM. Typical errors were Zn: $\pm$1.5 at.%, Mg: $\pm$3 at.% and RE: $\pm$0.5 at.%. The 0.5 cm^3 single quasicrystal of $Zn_{60}Mg_{31}Ho_9$ was obtained by the Bridgman method from the incongruent melt of $Zn_{46}Mg_{51}Ho_3$. Details of the crystal growth were published elsewhere [16].

The DC magnetic susceptibility was measured using a superconducting quantum interference device (SQUID) magnetometer (MPMS-XL, Quantum Design) in the temperature range 1.8 to 300 K. The field cooling and zero-field cooling runs were performed in the applied magnetic field of 100 Oe.

For neutron scattering experiments, samples were mounted in a standard ^{4}He refrigerator and cooled down to $T \simeq 1.3$ K. The single quasicrystal was oriented with its two-, three- or five-fold (2f, 3f or 5f) axis vertical so that the scattering plane coincides with the 2f, 3f, or 5f plane, respectively. The neutron scattering experiments were performed using the triple-axis spectrometer ISSP-GPTAS and multidetector diffractometer IMR-HERMES [17], installed at JRR-3M, JAERI (Tokai). The GPTAS was operated in the double-axis configuration, and collimations of 40'-80'-40' or 40'-80'-80' were employed. Incident neutrons of $k_i = 2.67$ Å^{-1} were selected by a vertically-focusing pyrolytic graphite (PG) monochromator, and second harmonics was eliminated by a PG filter. On the other hand for the HERMES, incident neutrons of $k_i = 3.45$ Å^{-1} were selected by a vertically-focusing germanium monochromator with 331 reflections used. Higher order contamination is negligible for this diffractometer.

3. Results and Discussion

First, we examined the microstructure and neutron diffraction pattern of the $Zn_{50}Mg_{42}Ho_8$ sample prepared under the same condition as the previous report [5]: as-solidified alloy was annealed under 873 K for 20 min and subsequently at 673 K for 48 h. We selected the RE=Ho system, because it exhibited the most prominent magnetic Bragg reflections in Ref. [10]. Shown in Fig. 1 are the back-scattering-electron image (BEI) and neutron diffraction pattern of the $Zn_{50}Mg_{42}Ho_8$ sample. Magnetic contribution in the diffraction pattern (Fig. 1(b)) was deduced from difference between the higher ($T = 20$ K) and lower ($T \simeq 1.5$ K) temperature data. As seen in the diffraction pattern, there appear sharp magnetic-Bragg-reflection peaks, in addition to broad diffuse scattering peaks. The diffraction pattern almost reproduces the previous results. However, the BEI micrograph apparently shows coexisting four phases, which are icosahedral $Zn_{57}Mg_{33}Ho_{10}$ phase, and three crystalline $(Zn_{1-x}Mg_x)_5Ho$, Zn_3Mg_7 and Mg phases. We noted that x for the crystalline $(Zn_{1-x}Mg_x)_5Ho$ phase fluctuates around $x \sim 0.2$. Since the former two phases contain rare-earth (magnetic) elements, both of them can have a possibility for the magnetic long-range order. Therefore one cannot conclude that the long-range order originates from the icosahedral phase.

In order to clarify the origin of the long-range order, we next investigated single phased alloys of the icosahedral and $(Zn_{1-x}Mg_x)_5Ho$ crystalline phases. The single phased $(Zn_{0.8}Mg_{0.2})_5Ho$ sample was obtained by annealing as-solidified alloy at 1023 K for 1 h and then 923 K for 20 h. The BEI micrograph of this sample is shown in Fig. 2(a). This shows that the sample consists of the crystalline phase with slight composition fluctuation. The neutron diffraction pattern is shown in Fig. 2(b). One can clearly see magnetic Bragg reflections, which appear at quite the same positions as those found in the previous report. In fact, one can index the Bragg reflections

with the quasicrystalline indices given in Ref. [10], as shown by the vertical lines in the figure. However, this is obviously misleading indexing, since the Bragg reflections originate from the crystalline phase, and not from the icosahedral phase. This accidental coincidence can be due to densely situated reflection positions in quasicrystals: one can index a peak at any position by a quasicrystalline index if intensity is not taken into account. The magnetic susceptibility of the crystalline phase is shown in Fig. 3. It clearly shows an anomaly at $T_{\rm N} = 7.4$ K. This temperature is almost equal to the ordering temperature (about 7 K for RE=Ho) in the previous report, confirming that the long-range order is from the crystalline contaminating phase.

The single icosahedral-phased sample was obtained by annealing the as-solidified $Zn_{60}Mg_{30}Ho_{10}$ alloy at 723 K for 200 h. The BEI micrograph and neutron diffraction pattern are shown in Fig. 4. The BEI micrograph confirms that the obtained alloy mainly consists of the icosahedral phase with a very small amount of the contaminating crystalline phase. The neutron diffraction pattern in Fig. 4(b) evidences absence of the magnetic long-range order in this sample. Instead, broad diffuse-scattering peaks were observed in the diffraction pattern at $|\boldsymbol{Q}_{\parallel}| \sim 0.55, 1.15, 2.0$Å^{-1}. This indicates that only short-range spin correlations develop at the lowest temperature in the Zn-Mg-Ho icosahedral quasicrystal. In view of the above results, it can be concluded that the previously-observed magnetic Bragg reflections (i.e., the long-range order) are due to the $(Zn_{0.8}Mg_{0.2})_5Ho$ crystalline phase contaminating the $Zn_{50}Mg_{42}Ho_8$ alloy.

We further prepared the $Zn_{50}Mg_{42}RE_8$ alloys for other RE elements, which are RE = Tb, Dy and Er. They were annealed under the same condition as that in Ref. [5]. The BEI micrographs of the resulting alloys are shown in Fig. 5. As seen in the figures, the crystalline phase largely remains in the RE=Tb sample, whereas for the RE=Dy and Er samples the crystalline phases almost diminish, even for the same annealing condition. This is consistent with the fact that the magnetic Bragg reflections were strongly observed in the RE = Ho and Tb alloys, and were obscure in the RE = Dy and Er samples in the previous report. Thus, this metallographic result also supports that the magnetic long-range order should be ascribed to the crystalline contaminating phase.

In the above we have shown that the long-range magnetic order is absent in the icosahedral quasicrystal, and that only the diffuse scattering evolves even at the lowest temperatures. On the other hand, as reported in Ref. [6], the magnetic susceptibility detects the spin-glass-like freezing at low temperatures, for example, $T_{\rm f} \sim 2$ K for RE = Ho. Hence, one should regard that the spins in the icosahedral quasicrystals freeze at the lowest temperatures with certain short-range spin correlations. Since the short-range correlations are intrinsic to the icosahedral quasicrystals, characteristics of the spin system in the quasiperiodic structure may possibly be elucidated by investigating the short-range correlations. We therefore observed the magnetic diffuse scattering over wide $\boldsymbol{Q}$-range using the Zn-Mg-Ho icosahedral single-quasicrystal, and tried to deduce whole characteristics of the associated short-range spin correlations.

The overall features of the diffuse scattering were obtained by measuring the magnetic scattering intensity for the 2f, 3f, and 5f planes [15]. For the 2f plane, the triple-axis spectrometer GPTAS was used, whereas for the 3f and 5f planes, the experiments were carried out at the multidetector diffractometer HERMES. The measurements were made at two temperatures $T \simeq 1.3$ K and $T = 20$ K. Then, the magnetic scattering was deduced by the difference $I(T \simeq 1.3\ {\rm K}) - I(T = 20\ {\rm K})$. We observed the magnetic scattering in a doubled symmetrically-independent-region in each plane, which will be shown in Fig. 6 by solid lines. We confirmed that the magnetic scattering in the two independent regions is identical. Then the data were folded into a single independent region to increase the statistical precision, and they were again unfolded to the full circle to improve the visibility of the symmetric features.

The obtained magnetic-scattering-intensity maps are shown in Figs. 6(a), 6(b) and 6(c) for the 2f, 3f and 5f planes, respectively. As seen in the figures, the magnetic scattering is not spherical, but is highly structured with a number of spot-like peaks connected by weak diffuse-scattering ridges. The spots-like peaks do not correspond to magnetic Bragg reflections, as evidenced by their finite widths [14]. The correlation length was estimated from the peak widths at $\boldsymbol{Q}_{\parallel} = (0, 0.55, 0)$ as $\xi \sim 10$ Å in half width at half maximum (HWHM). The positions of the intense nuclear Bragg reflections are also shown by white dots in the first quadrant of Fig. 6. By comparing them with the diffuse-scattering patterns, one can easily see that the diffuse scattering appears where the intense nuclear Bragg reflections are absent. Thus the spin correlations are dominantly antiferromagnetic, which is consistent with the magnetic susceptibility [4].

Since the magnetic scattering mainly consists of the spot-like peaks, it is inferred that the associated spin correlations are described by certain modulation vectors. As is well established now, structure of icosahedral quasicrystals can be described by projection of a periodic crystal in six-dimensional (6D) space. Consequently, the nuclear Bragg reflections are indexed by sets of six integers. By an analogy of this indexing, one may expect that the

magnetic diffuse scattering can be described by certain 6D modulation vectors. In fact, by calculating magnetic scattering intensity from model spin correlations with 6D modulation vectors, we have found that the observed intensity maps are coherently reproduced using the single modulation vector $\boldsymbol{Q} = (\frac{3}{4}, 0, 0, \frac{1}{2}, \frac{3}{4}, \frac{1}{2})$ [15]. The result that the observed diffuse-scattering can be described using the single 6D modulation vector suggests that the associated short-range spin correlations may be closely related to the hidden translational-symmetry of the quasiperiodic structure in the 6D space. Finally, we have to note that the quasi-five-dimensional modulation, which was suggested solely from the 2f plane results in our earlier paper [14], cannot reproduce the observation in the 3f and 5f planes.

4. Conclusions

The magnetic order in the Zn-Mg-RE systems has been carefully reinvestigated by the magnetic susceptibility and neutron diffraction, with the aid of the metallographic techniques. It was found that the icosahedral phases ($Zn_{60}Mg_{30}RE_{10}$) do not exhibit any magnetic long-range order but show only the development of short-range spin correlations even at the lowest temperatures. The previously-reported long-range order was ascribed to the $(Zn_{1-x}Mg_x)_5RE$ crystalline phases, which can be a contaminant of the previously-used $Zn_{50}Mg_{42}RE_8$ alloys. The short-range spin correlations have been investigated using single-quasicrystal neutron scattering. The observed spin correlations were found to be described by a single 6D modulation vector. This may be an unique characteristic of the quasicrystalline magnetism, reflecting the hidden 6D translational-symmetry of the icosahedral quasicrystals.

5. ACKNOWLEDGEMENTS

The present authors thank Drs. E. Abe, L. H. Tang, I. R. Fisher, A. Mishchenko and S. Matsuo for valuable discussions, and Drs. T. Ishimasa and B. Charrier for providing us with their results prior to publication.

References

[1] Z. Luo, S. Zhang, Y. Tang and D. Zhao, Scripta Metal. Mater. **28**, 1513 (1993).

[2] A. Niikura, A. P. Tsai, A. Inoue and T. Masumoto, Philos. Mag. Lett. **69**, 351 (1994).

[3] A. P. Tsai, A. Niikura, A. Inoue, T. Masumoto, Y. Nishida, K. Tsuda and M. Tanaka, Philos. Mag. Lett. **70**, 169 (1994).

[4] Y. Hattori, A. Niikura, A. P. Tsai, A. Inoue, T. Masumoto, K. Fukamichi, H. Aruga-Katori and T. Goto, J. Phys.: Condens. Matter **7**, 2313 (1995).

[5] B. Charrier and D. Schmitt, J. Magn. Magn. Mater. **171**, 106 (1997).

[6] I. R. Fisher, K. O. Cheon, A. F. Panchula, P. C. Canfield, M. Chernikov, H. R. Ott and K. Dennis, Phys. Rev. B **59**, 308 (1999).

[7] S. Kashimoto, S. Matsuo, H. Nakano, T. Shimizu and T. Ishimasa, Solid State Commun. **109**, 63 (1999).

[8] B. Charrier and D. Schmitt, J. Magn. Magn. Mater. **189**, 165 (1998).

[9] D. R. Noakes, G. M. Kalvius, R. Wäppling, C. E. Stronach, M. F. White Jr., H. Saito and K. Fukamichi, Phys. Lett. A **238**, 197 (1998).

[10] B. Charrier, B. Ouladdiaf and D. Schmitt, Phys. Rev. Lett. **78**, 4637 (1997). The magnetic modulation-vector defined in this paper can be rewritten as $\boldsymbol{q} = (\frac{1}{2}, 0, 0, 0, 0, 0)$ using the present definition [15].

[11] A. P. Tsai, A. Niikura, A. Inoue and T. Masumoto, J. Mater. Res. **12**, 1468 (1997).

[12] A. Langsdorf, F. Ritter and W. Assmus, Philos. Mag. Lett. **75**, 381 (1997).

[13] Z. Islam, I. R. Fisher, J. Zarestky, P. C. Canfield, C. Stassis and A. I. Goldman, Phys. Rev. B **57**, R11047 (1998).

[14] T. J. Sato, H. Takakura, A. P. Tsai and K. Shibata, Phys. Rev. Lett. **81**, 2364 (1998)

[15] T. J. Sato, H. Takakura, A. P. Tsai, K. Ohoyama, K. Shibata and K. H. Andersen, *Materials Research Society Symposium Proceedings Volume 553: Quasicrystals*, edited by J. M Dubois, P. A. Thiel, A. P. Tsai and K. Urban (Materials Research Society, Pennsylvania, 1999) p. 415; T. J. Sato, H. Takakura, A. P. Tsai, K. Ohoyama, K. Shibata and K. H. Andersen (submitted).

[16] T. J. Sato, H. Takakura and A. P. Tsai, Jpn. J. Appl. Phys. **37**, L663 (1998).

[17] K. Ohoyama, T. Kanouchi, K. Nemoto, M. Ohashi, T. Kajitani and Y. Yamaguchi, Jpn. J. Appl. Phys. **37**, 3319 (1998).

Figures

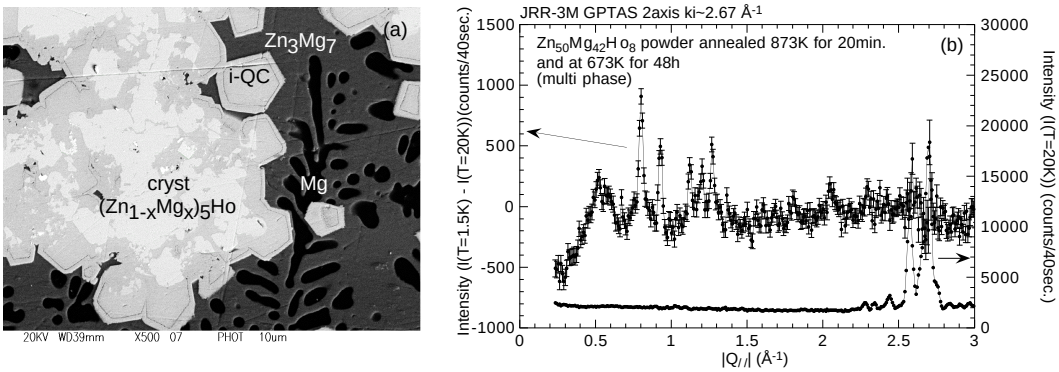

Fig.1 T.J.Sato et al.

Fig. 1. Fig. 1: (a) BEI micrograph and (b) neutron diffraction pattern of the $Zn_{50}Mg_{42}Ho_8$ alloy annealed at 873 K for 20 min and then 673 K for 48 h. In (b), magnetic contribution was deduced from the temperature difference (see text for details).

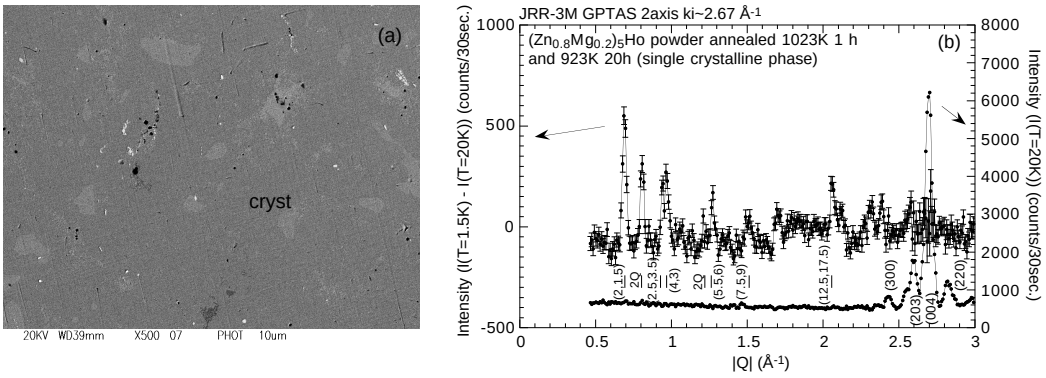

Fig.2 T.J.Sato et al.

Fig. 2. Fig. 2: (a) BEI micrograph and (b) neutron diffraction pattern of the crystalline (hexagonal) $(Zn_{0.8}Mg_{0.2})_5Ho$ alloy annealed at 1023 K for 1 h and then 923 K for 20 h. In (b), magnetic contribution was deduced from the temperature difference (see text for details).

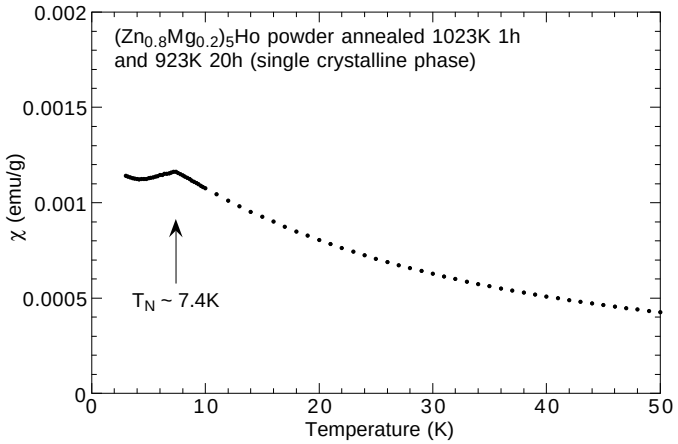

Fig. 3. Fig. 3: Magnetic susceptibility of the crystalline $(Zn_{0.8}Mg_{0.2})_5Ho$ alloy annealed at 1023 K for 1 h and then 923 K for 20 h.

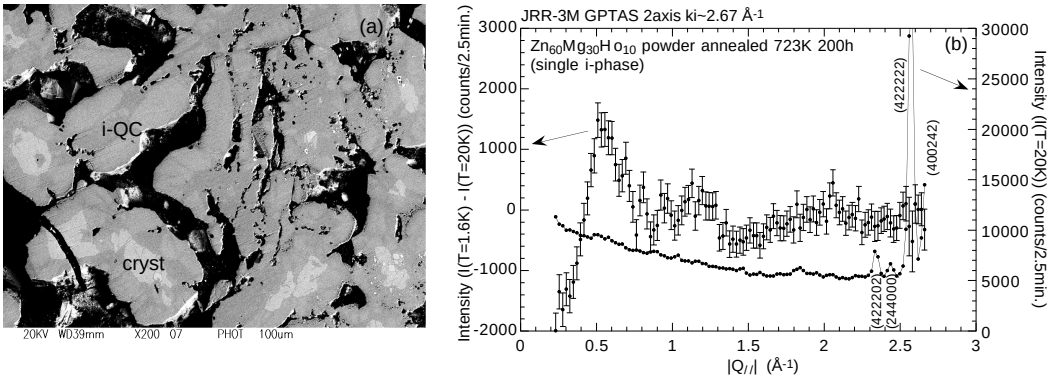

Fig.4 T.J.Sato et al.

Fig. 4. Fig. 4: (a) BEI micrograph and (b) neutron diffraction pattern of the icosahedral $Zn_{60}Mg_{30}Ho_{10}$ alloy annealed at 723 K for 200 h. In (a), black regions are holes. In (b), magnetic contribution was deduced from the temperature difference (see text for details).

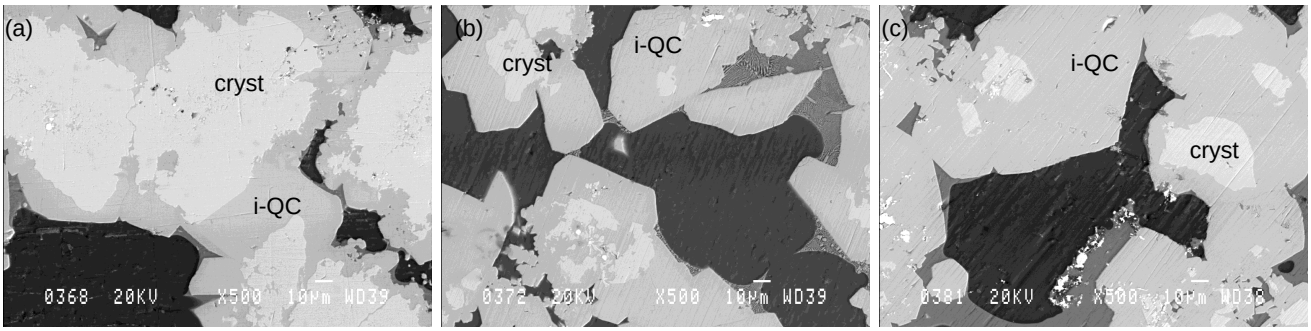

Fig.5 T.J.Sato et al.

Fig. 5. Fig. 5: BEI micrographs of the $Zn_{50}Mg_{42}RE_8$ alloys annealed at 873 K for 20 min and then 673 K for 48 h. RE = (a) Tb, (b) Dy and (c) Er.

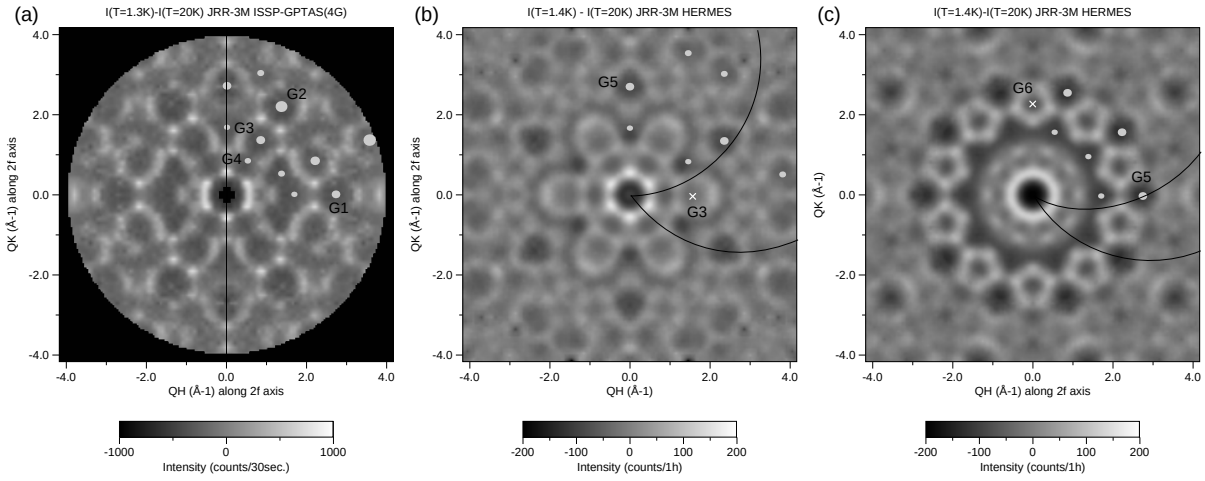

Fig. 6 T.J. Sato et al.

Fig. 6. Fig. 6: Magnetic-scattering-intensity maps for the (a) 2f, (b) 3f and (c) 5f planes of the icosahedral Zn-Mg-Ho single quasicrystal. Magnetic contribution was deduced from the temperature difference (see text for details). The white dots are the in-plane intense nuclear-Bragg-reflection positions, whereas the white crosses are the intense Bragg reflections that are in vicinity of the corresponding scattering planes. The data are taken only in the regions between the two solid lines.